energies

MDPI

Article

Reliability and Availability Optimization of Smart Microgrid Using Specific Configuration of Renewable Resources and Considering Subcomponent Faults

Geeta Yadav [1,*], Dheeraj Joshi [2], Leena Gopinath [1] and Mahendra Kumar Soni [1]

[1] Manav Rachna International Institute of Research and Studies (MRIIRS), Faridabad 121004, India
[2] Department of Electrical Engineering, Delhi Technological University, Delhi 110042, India
* Correspondence: gt.yadav@gmail.com; Tel.: +91-9958-111-454

Abstract: In this paper, renewable resources, namely photovoltaic panels (PV), are placed in a specific configuration to obtain the maximum reliability and availability of a microgrid and study the subcomponent-level reliability and availability. The reliability of components can be increased by trying different configurations of the components. We identify the preferred configuration used for the PV panels as bridged linked. The overall reliability of the microgrid is increased when component-wise reliability is considered. Even components are further divided into subcomponents, and the multiple faults of each component are considered. The method used for the reliability evaluation and availability study is Markov state transition modeling. The microgrid's reliability and availability are plotted concerning time using Matlab. The optimization of reliability and availability is conducted through optimization techniques such as the genetic algorithm (GA) and artificial neural networks (ANN). The results are compared and validated for the optimal values of mean time to failure (MTTF) and mean time to repair (MTTR). Using a genetic algorithm, there is a 96% of improvement in the reliability, and after applying the neural networks, a significant improvement of 97% along with quick results is achieved.

Keywords: microgrid; reliability; bridge-linked configuration; failure rate; Markov model; state transition diagram

Citation: Yadav, G.; Joshi, D.; Gopinath, L.; Soni, M.K. Reliability and Availability Optimization of Smart Microgrid Using Specific Configuration of Renewable Resources and Considering Subcomponent Faults. *Energies* **2022**, *15*, 5994. https://doi.org/10.3390/en15165994

Academic Editor: Jeyraj Selvaraj

Received: 12 July 2022
Accepted: 16 August 2022
Published: 18 August 2022

1. Introduction

The microgrid adds distributed energy resources with advanced power electronic interface modules along with utility grid connections for serving local loads [1]. It also adds digital, control, advanced operations, and advanced resources to the electrical grid. Many changes are needed in the existing legacy electrical grid, including adding renewable resources at generation, adding smart appliances at consumption, and the addition of new technologies, such as smart meters, IoT, scheduling, cronjobs, etc. [1]. The smart grid needs to be energy-efficient, reliable, and secure in the same way as the existing electrical grid despite having new changes from new technologies and optimizations [2]. The technologies applied for the smart grid are still in the process of real world implementation [2]. There are a lot of challenges to their implementations, such as the two-way flow of information, adding renewable resources, adding smart appliances on the consumer side, the reliability and cost effectiveness of the flow of information, and self-healing. The idea to replace the existing system with a new, improved, and optimized smart power grid infrastructure presents multiple challenges and threats to effectively integrating smartness without impacting the use of the existing grid. The various indices for visualizing the performance of the integrated system are energy efficiency, reliability, security, and flexibility. The electricity generation at the consumer end is done through renewable sources.

The year 2021 is considered the dark year of electricity due to longer duration power cuts or blackouts or brownouts all across the world [3]. There were two transmission

line failures that happened in Mexico in January 2021, with blackouts in one-third of the country [3]. In the same month and year, Pakistan faced a technical fault in the Guddu thermal plant, which is at the center of the Pakistan grid, causing a cascading blackout across the whole country. Similarly, Winter Storm Uri in Japan in February 2021 caused a complete shutdown of 10 GW of a thermal power plant. A technical issue on main transmission lines between Prestea and Obuasi caused a national power outage in Ghana on 7 March according to grid operator GRIDCo. After a trip to the 4.3 GW coal-fired Hsinta Power Plant in the southern city of Kaohsiung, several cities in Taiwan, including the capital Taipei, experienced rolling blackouts in May 2021. Jordan was likewise hit by a widespread power outage on 21 May. China was confronted with yet another electricity shortage. Thus, to reduce the impacts of electrical failures, we need to study reliability and availability thoroughly. This is all about the world, but when we consider Indian rural areas, people are still receiving electricity for only a few hours although they have enough renewable resources are wasting till this concept came into mind.

Various methodologies, such as the intelligent state space pruning with a local search for the evaluation of power system reliability, are used to assess the smart grid's reliability. This novel method is utilized to assess the smart grid's reliability, as are numerous optimization techniques such as PSO [4]. Multiple publications on the reliability of smart grid components have been published where only component-level reliability is considered. The interconnected optimum filtering issue for distributed dynamic state estimation considering packet losses is used in the smart grid to estimate dispersed states via unreliable communication networks [5]. The component's reliabilities are used to assess the reliability. In a smart grid, different components are used, as well as multiple modes of operation. Because PV panels are inexpensive, they are commonly employed as a solar energy source. PV panels can operate in two modes: redundancy and parallel. The DC to DC converters are used to calculate the system's reliability when renewable resources are blended, such as solar panels and wind turbines. MPPT and MTTF, or maximum power point tracking and maximum time to transfer, are two indexes used to determine a system's reliability. To boost DC to DC converters using PV, the reliability is computed using both performance indices [6]. Reliability evaluation of distributed networks has been performed in multiple papers where a specific component is studied and reliability was evaluated for a superconducting fault current limiter (SFCL) [7]. Similarly, there are multiple papers where component reliability parameters are studied; for example, solar farm generation has been investigated using the Markov chain model [8]. Reliability was evaluated for a microgrid using a chronological Monte Carlo simulation with Markov switching modeling. A standard system was taken, and the performance indices of MTTR and MTTF were evaluated, showing very little improvement [9]. Robustness is optimized in interconnected microgrids using nash bargaining [10]. To study the uncertainty in the model, multiple robust control techniques have been applied and optimized [11]. Robustness is how strong the model is in case of any uncertainty due to renewable resources. There are multiple indices for visualizing the performance of microgrids: energy efficiency, reliability, security, flexibility, robustness, self-healing and demand-supply fulfillment. The demand and supply gap should be fulfilled by distributors and retailers through planned strategies [12].

Using the methods described, in this paper, different configurations are used to evaluate the best values of reliability and availability using Markov modeling and again optimized using GA and ANN. The economic progress of developing countries such as India is strongly reliant on the reliability and prominence of their electric power supply. There can be many ways to arrange the components, such as in series, in parallel, in series parallel, cross-linked, etc., but the best possible way is not thoroughly explained in most reliability studies; therefore, we have considered that point in this study. This paper worked on the below points: (a) component-level microgrid reliability was convoluted by many researchers, but the effect of all the components has not been studied in any of the papers which are worked on in this paper. Subcomponent configuration level studies have not been performed yet; (b) an assessment of the reliability and availability at the component level

and the level of the overall microgrid is performed in this paper using Markov modeling; (c) the application of optimization techniques to increase reliability and availability is a new area explored in this paper.

When designing any microgrid, design parameters play a crucial role in determining reliability as well as availability based on the mean time to failure and repair, which are calculated by failure rates. Any grid can be divided into generation systems, distribution systems, transmission systems, and customer systems. Very few papers considered the reliability of the overall grid. Most papers worked on the assesmsment of the reliability of the distribution system [13]. To evaluate the reliability, multiple parameters are considered; for example, mean time to failure and mean time to repair [14] of the different components are modeled, which are taken from the literature [13]. The average system unavailability index (ASUI), system average interruption frequency index (SAIFI), system average interruption duration index (SAIDI), customer average interruption duration index (CAIDI), ref. [15] and other indices are used to assess microgrid dependability. The most widely used renewable resource is solar power, and there are multiple papers where the reliability of solar generation is studied thoroughly. Furthermore, its applications for the evaluation of generation performance with different profiles are considered [16]. People around the world are highly interested in incorporating renewable resources into the existing grid to increase the performance of the grid with better environmental impacts. Thus, researchers around the world study different models of grids in different areas [16]. The evaluations are different for every researcher, as the localities considered are different, but the reliability curve is almost the same concerning time across the globe [16]. This paper has considered the solar profile of Bhiwani, Haryana, India.

Section 2 contains the proposed approach explained along with the component-wise description discussed in Section 3. Section 4 contains the Markov modeling method explained in detail, along with the state transition matrix. The results and discussions are covered in Section 5. Conclusions are mentioned in Section 6.

2. Research Method

There are multiple components that are used which are connected with different configurations, which can improve or decrease the reliability of the microgrid. Thus, it is equally important to discuss the component-level reliability and configuration-based reliability of the microgrid. To estimate the reliability of the microgrid [17], the failure rate of the manufacturer needs to be considered, as well as how to best use it in the best configuration to optimize the reliability of the microgrid. Multiple PV panels are used with other components of the microgrid with different configurations, such as in series, in parallel, in series-parallel, cross-linked, bridge-linked, and cross-tied [18]. The reliability of PV panels is computed based on the configuration it is arranged in, and the failure rate of each panel is considered. From the estimate of the reliability of PV panels, the overall failure rate of PV panels is computed and combined with the converter. These two components are more focused upon in this study, where PV panels and converters are combined as a single unit, and Markov modeling is performed based on different states at different points of time. The components considered a part of the microgrid in this study are PV panels, converters, transformers, and load, as shown in Figure 1.

The reliability of PV panels was computed first. The PV panels were connected in a bridge-linked configuration, where every panel's reliability, i.e., cell reliability was considered. Using Equations (1), the overall PV panel reliability was computed. Similarly, the reliability of every component, such as converters and transformers, was computed using different states of the microgrid. Based on different states, reliability is again computed using the Markov reliability model, and the overall reliability and availability of the microgrid were evaluated. The different modes that were also considered are a success (i.e., a good state), failure mode (i.e., component failure), repair mode (i.e., the component being in a repair state), and maintenance mode (the regular check of components after a specific duration). Then, the same model is simulated through a genetic algorithm as

well as artificial neural networks to obtain better results of mean time to failure (MTTF) for microgrid reliability. The component level reliability and availability are calculated, so every component is discussed below. The flow chart to compute reliability is shown in Figure 2.

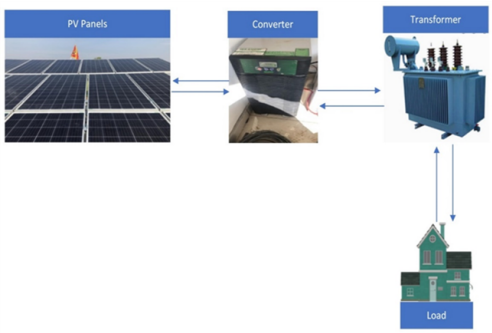

Figure 1. Transition diagram of proposed microgrid model.

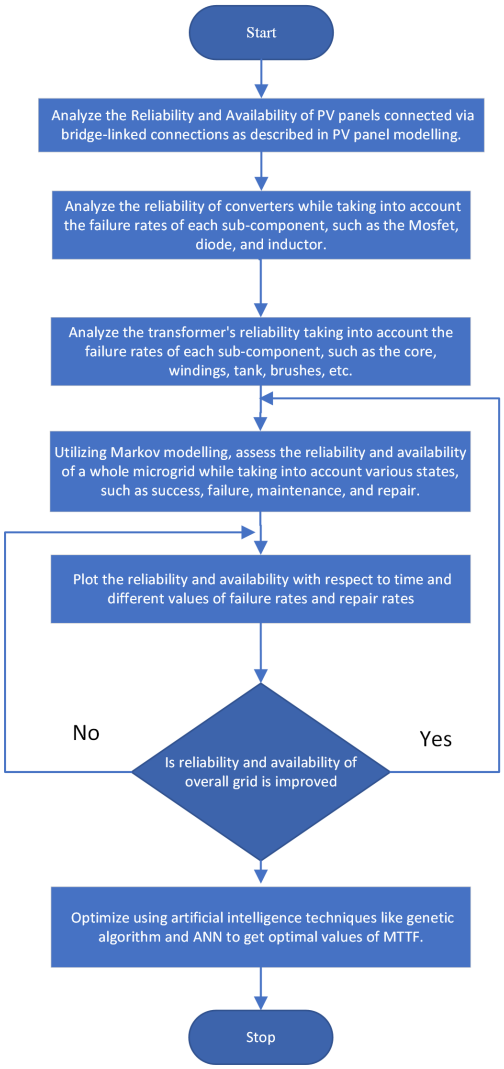

Figure 2. Flow chart of proposed methodology.

3. Model Development of Each Component

3.1. Bridge-Linked PV Panels

PV panels are the first components in the microgrid's overall construction. If the PV panels are connected in series, the voltage level is increased, but the current remains the

same. The PV panels can be connected in parallel, for which the current will increase but the voltage will remain the same. To solve this problem, two other configurations are tried: series parallel and cross-tied configurations. In the series parallel configuration, the power increases. Here in this paper, we have considered the lifetime of PV panels when they are in the active state [18]. When the reliability is evaluated for these systems, the best configuration is considered based on the operational lifetime of the networks [18]. The operational lifetime is maxed when the bridge-linked array is used. Thus, we used bridge-linked connections between solar cells [19] as shown in Figure 3. The dotted lines show multiple panels connected in a bridge shape. Abbreviations are mentioned in the last section.

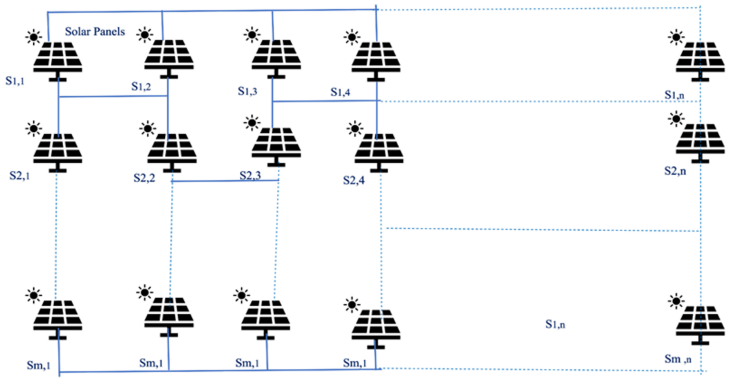

Figure 3. Bridge-linked PV panel configuration.

Equation (1) demonstrates the mathematical formula for solar PV panels:

$$R_{PV}(\tau) = 1 - \left(\sum_{x=1}^{m} \left((1 - R_{mod_{xy}}(\tau))^n \right) \right) \quad (1)$$

From this reliability, the failure rate of the PV panels can be calculated. The function considered is concerning density and calculated using probability theory. The parameter x is the number of PV panels in rows, and y is the number of PV panels in columns. The function is evaluated based on the active time of the components considered. The chance of failure for the time interval $[t, t + \tau]$ is given in Equation (1). The mean time to failure is calculated with probability theory, where the condition is that the components would not fail until time t.

3.2. Converters

There are multiple papers where converters are studied and the reliability of converters is estimated based on the mode of use [17,20]. The interleaved boost converter has multiple stages with a diode, inductor, and switch in each stage [21]. In this paper, the reliability of the converter is calculated and connected with PV panels as shown below, where subcomponents of the boost converter have similar failure rates [20,22] calculated from Equations (5)–(7) [23]. The failure rate of subcomponents MOSFET, diode, and inductor are shown in Equations (2)–(4), respectively. Abbreviations are mentioned in the last section.

$$\lambda_L = \lambda_{MOSFET} = \lambda_b \, \pi_T \, \pi_A \, \pi_Q \, \pi_E \quad (2)$$

$$\lambda_D = \lambda_{Diode} = \lambda_b \pi_T \pi_S \pi_C \pi_Q \pi_E \quad (3)$$

$$\lambda_Q = \lambda_{Inductor} = \lambda_b \, \pi_T \, \pi_Q \, \pi_E \quad (4)$$

Mosfet

$$\pi_T = \exp\left[-1925 \left(\frac{1}{T_j + 273} - \frac{1}{298} \right) \right] \quad (5)$$

Diode

$$\pi_T = \exp\left[-3091\left(\frac{1}{T_j + 273} - \frac{1}{298}\right)\right] \tag{6}$$

Inductor

$$\pi_T = \exp\left[\frac{-0.11}{8.617 \times 10^{-5}}\left(\frac{1}{T_{HS} + 273} - \frac{1}{298}\right)\right] \tag{7}$$

The reliability of the converter is calculated based on the below formula in Equation (8):

$$R^{1-2}(t) = e^{-\lambda t} + \lambda\, P_R t e^{-\lambda t} \tag{8}$$

The failure rates of inductor, diode, and MOSFET are as follows in Equation (9):

$$\lambda_1 = \lambda_2 = \lambda_3 = \lambda_L + \lambda_D + \lambda_Q \tag{9}$$

The overall failure rate of the converter is calculated based on the reliability calculated above.

$$R(t) = e^{-\int_0^{t1} \lambda(t)\mathrm{dt}} \tag{10}$$

Using the above formula, the failure rate of the converter is calculated from Equation (10).

3.3. Transformer

The transformer is made up of nine components [24]: a core, winding, tank, oil insulation, solid insulation, bushing, tap-changer, cooling pump and cooling fan [24]. The unwavering mass submodel was originally evolved for each part individually and finally incorporated into the general reliability model of the transformer [24]. S. No.1 to 9 in Table 1 shows the reliability functions for submodels of the transformer. The transformer has eight submodels, as shown in Table 1. λ_c, λ_W, λ_T, λ_0, λ_{SI}, λ_B, λ_{TC}, λ_P and λ_{CF} are the failure rates of the submodels, i.e., the core, winding, tank, oil coating, solid coating or insulation, bushing, tap-changer, cooling pump and cooling fan, respectively. R_c, R_W, R_T, R_O, R_{SI}, R_B, R_{TC}, R_P and R_{CF} are the reliabilities of the core, winding, tank, coil coating, solid coating or insulation, bushing, tap-changer, cooling pump and cooling fan, respectively. Information about assorted reliability is enlisted as follows. Abbreviations are mentioned in the last section.

When the cooling fan and oil pump are running, the transformer is loaded to its maximum capacity. However, if any of these pumps and cooling fans [24] fail, the transformer can still run with less load. Therefore, a parallel reliability structure of the cooling system reliability model [24] is constructed, calculating the reliability when both the pump and the fan are [24] operating normally or when one of the components fails [25]. If (λ_P) is the failure rate of an oil pump, then the reliability (R_p) [24] of the oil pump is measured as from Equation (11).

$$R_p(t) = e^{-\int_0^t \lambda_p(\tau)d\tau} \tag{11}$$

If λ_{CF} is the failure rate of fans [24] which cools, then the cooling [24] fan's reliability (R_{CF}) is measured by Equation (12).

$$R_{CF}(t) = e^{-\int_0^t \lambda_{CF}(\tau)d\tau} \tag{12}$$

The overall cooling system's reliability (R_{CS}) is measured from Equation (13).

$$R_{CS} = 1 - (1 - R_P R_{CF})(1 - R_P)(1 - R_{CF}) \tag{13}$$

The numerical articulation for complete reliability of subsystems (R_{MAN}) is communicated by Equation (14).

$$R_{MAN} = R_C R_W R_T R_O R_{SI} R_B \tag{14}$$

Finally, the articulation for total transformer reliability (R_{TXR}) is given as [24] in Equation (15).

$$R_{TXR} = R_{MAN} R_{CS} R_{TC} \tag{15}$$

Table 1. Reliability submodels of transformer.

S. No.	Component Name	Failure Modes	Reliability Functions for Submodels
1	Core	The core lamination, core joints, and lamination gaps were found to be the most common causes of core failure [24].	$R_c(t) = e^{-\int_0^t \lambda_c(\tau)\mathrm{d}\tau}$
2	Winding	A normal winding non-success occurs when the coating on the winding fails owing to widespread or local overheating [24].	$R_W(t) = e^{-\int_0^t \lambda_W(\tau)\mathrm{d}\tau}$
3	Tank	The high pressure in a transformer's tank caused by gases, as well as corrosion caused by moisture and aging, are the main causes of the tank's failure [25].	$R_T(t) = e^{-\int_0^t \lambda_T(\tau)\mathrm{d}\tau}$
4	Oil Coating	The main causes are partial discharge and moisture infiltration; other causes include suspended particles in oil and arcing [24].	$R_O(t) = e^{-\int_0^t \lambda_0(\tau)\mathrm{d}\tau}$
5	Solid Coating	Insulation failure is primarily caused by short circuiting or cellulose aging, according to the electrical survey [24].	$R_{SI}(t) = e^{-\int_0^t \lambda_{SI}(\tau)\mathrm{d}\tau}$
6	Bushing	Overheating and insulation failure cause failure due to dust, water infiltration, and effects on the bushing.	$R_B(t) = e^{-\int_0^t \lambda_B(\tau)\mathrm{d}\tau}$
7	Tap-changer	Its operation is mechanical, which means it could break down. Other problems could be caused by motor drives or contact cooking [24].	$R_{TC}(t) = e^{-\int_0^t \lambda_{TC}(\tau)\mathrm{d}\tau}$
8	Cooling Pump		$R_P(t) = e^{-\int_0^t \lambda_P(\tau)\mathrm{d}\tau}$
9	Cooling Fan		$R_{CF}(t) = e^{-\int_0^t \lambda_{CF}(\tau)\mathrm{d}\tau}$

4. Markov Modeling

The microgrid consists of multiple components and multiple states, such as good, repair, failure, and maintenance states [17]. There will be 3n conditions of the parts of the microgrid. After time passed the working t, every component of the microgrid can be in a failure state [26] in the following time frame, Δt [27]. If the failure is detected, the component can be repaired, and if the failure is not detected, then it can be repaired only in maintenance mode. The λ, mean failure rate, μ_c recovery rate, and μ_p maintenance rate can be constant [24]. The state change of the components will change the state of the microgrid with the state probability transition. The system state changes from an i to a j state when a failure is found, as shown below in Equation (16). Abbreviations are mentioned in the last section.

$$Pij = \lambda_k \times \Delta t \times C \tag{16}$$

If non-success i.e., failure, is not found, Equation (17) is used.

$$Pij = \lambda_K \times \Delta t \times (1 - C) \tag{17}$$

After repairing the component, the component will be in a normal state (i.e., a good state), as shown in Equation (18).

$$Pij = \mu_{Ck} \times \Delta t \tag{18}$$

After a failure is not captured and repaired through maintenance through Equation (19).

$$Pij = \mu_{pk} \times \Delta t \tag{19}$$

The microgrid has two components, i.e., PV panels and converters. Each component can be in one of the three states: bood (G), non-success (F), or repair (R) [26]. Each component can be moved from a good state to a failure state, a failure state to a repair state, and vice versa, but not from a good to a repair state [19]. A two-component system with three states is explained below, and a similar approach has been used for a three-component system, for which results are shown in this paper. Since a three-component system is very complex to explain in this paper, the two-component system is explained below, but the same approach has been used in this paper for the three-component system [21]. When the system is in an optimal state, that means it is in a GG state [24]; after Δt, it can be moved to any of the following states. GF: if a non-success on the next component is found, then the state change is $P = \lambda_2 \Delta tc$ [17]. FG: if a non-success on the Ist component is found [26], then the state change is $P = \lambda_1 \Delta tc$. GR: if the system did not identify the non-success on the next component, the state change probability is: $P = \lambda_2 \Delta t(1-c)$. RG: if the model did not identify the non-success on the Ist element, then $P = \lambda_1 \Delta t(1-c)$ [24]. GG: this state is still present in the same condition with $P = 1-(\lambda_1+\lambda_2)\Delta t$. Similarly, for the next interval of time Δt, GF will be moved to any of the below states. If the 2nd component is mended, then the model will be back to good condition, GG, with probability $P = \mu_C 2\Delta t$. If the first component fails and failure is found, the system will move to the FF state with probability [28] $P = \lambda_1 \Delta tc$. If the system did not found a non-success on the 1st component, then $P = \lambda_1 \Delta t(1-c)$, and the remainng terms are calculated similarly. The state transition diagram of the microgrid model shown in Figure 1 is depicted in Figure 4 below.

The A matrix shown below is the state transition matrix. Using this matrix, the reliability [29] of the microgrid is calculated concerning time [29].

$$A = \begin{pmatrix}
1-(\lambda_1+\lambda_2)\Delta t & \mu_{C2}\Delta t & \mu_{p1}\Delta t & \mu_{C2}\Delta t & 0 & 0 & \mu_{p2}\Delta t & 0 & 0 \\
\lambda_1 C\Delta t & 1-(\lambda_2+\mu_{C1})\Delta t & 0 & 0 & \mu_{C2}\Delta t & 0 & 0 & \mu_{p2}\Delta t & 0 \\
\lambda_1(1-C)\Delta t & 0 & 1-(\lambda_2+\mu_{p1})\Delta t & 0 & 0 & \mu_{C2}\Delta t & 0 & 0 & \mu_{p2}\Delta t \\
\lambda_2 C\Delta t & 0 & 0 & 1-(\lambda_1+\mu_{C2})\Delta t & \mu_{C1}\Delta t & \mu_{p1}\Delta t & 0 & 0 & 0 \\
0 & \lambda_2 C\Delta t & 0 & \lambda_1 C\Delta t & 1-(\mu_{C2}+\mu_{C1})\Delta t & 0 & 0 & 0 & 0 \\
0 & \lambda_2 C\Delta t & 0 & \lambda_1 C\Delta t & 1-(\mu_{C2}+\mu_{C1})\Delta t & 0 & 0 & 0 & 0 \\
0 & 0 & \lambda_2 C\Delta t & \lambda_1(1-C)\Delta t & 0 & 1-(\mu_{C2}+\mu_{p1})\Delta t & 0 & 0 & 0 \\
\lambda_2(1-C)\Delta t & 0 & 0 & 0 & 0 & 0 & 1-(\lambda_1+\mu_{p2})\Delta t\mu_{C1}\Delta t & \mu_{p1}\Delta t & 0 \\
0 & \lambda_2(1-C)\Delta t & 0 & 0 & 0 & 0 & \lambda_1 C\Delta t & 1-(\mu_{C1}+\mu_{p2})\Delta t & 0 \\
0 & 0 & \lambda_2(1-C)\Delta t & 0 & 0 & 0 & \lambda_1(1-C)\Delta t & 0 & 1-(\mu_{p2}+\mu_{p1})\Delta t
\end{pmatrix}$$

Using the above approach, the reliability of a microgrid is calculated as shown below in the results. Similarly, the approach with which availability is evaluated is explained below.

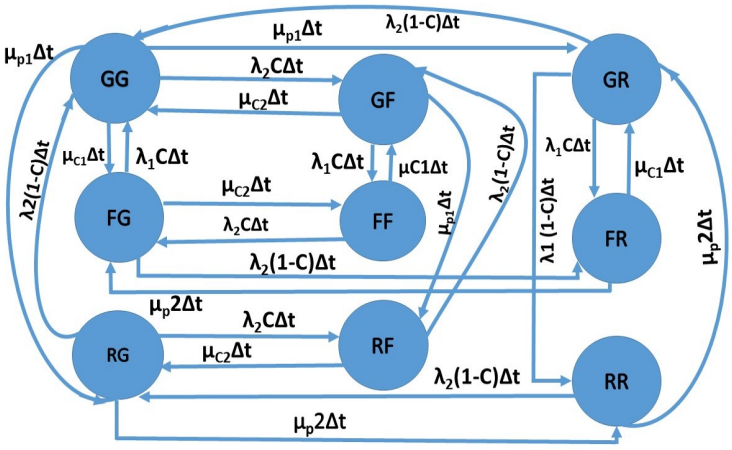

Figure 4. Transition diagram of proposed microgrid model.

5. Availability

The mathematical modeling of availability is done using a probabilistic [24] approach and difference differential equations [24]. These equations are solved for steady-state conditions. Probabilistic considerations give the following differential equations associated with the microgrid [30], as shown in Equations (20)–(29). Abbreviations are mentioned in the last section.

$$P = \dot{A}P \tag{20}$$

$$P'_{GG}(t+\Delta t) = P'_{GG}(t) - (\lambda_1+\lambda_2)P_{GG}(t) + \mu_{c1}P_{GF}(t) + \mu_{p1}P_{RG}(t) + \mu_{c2}P_{FG}(t) + \mu_{p2}P_{GR}(t) \tag{21}$$

$$P'_{GF}(t+\Delta t) = \lambda_1 CP_{GG}(t) + P'_{GF}(t) - (\lambda_2+\mu_{c1})P_{GF}(t) + \mu_{c2}P_{FF}(t) + \mu_{p2}P_{FR}(t); \tag{22}$$

$$P'_{RG}(t+\Delta t) = \lambda_1(1-C)P_{GG}(t) + P'_{RG}(t) - (\lambda_2+\mu_{p1})P_{RG}(t) + \mu_{c2}P_{RF}(t) + \mu_{p2}P_{RR}(t); \tag{23}$$

$$P'_{FG}(t+\Delta t) = \lambda_2 CP_{GG}(t) + P'_{FG}(t) - (\lambda_1+\mu_{c2})P_{FG}(t) + \mu_{c1}P_{FF}(t) + \mu_{p1}P_{RF}(t); \tag{24}$$

$$P'_{FF}(t+\Delta t) = \lambda_2 CP_{GF}(t) + \lambda_1 CP_{FG}(t) + P'_{FF}(t) - (\mu_{c2}+\mu_{c1})P_{FF}(t); \tag{25}$$

$$P'_{RF}(t+\Delta t) = \lambda_2 CP_{RG}(t) + \lambda_1(1-C)P_{FG}(t) + P'_{RF}(t) - (\mu_{c2}+\mu_{p1})P_{RF}(t); \tag{26}$$

$$P'_{GR}(t+\Delta t) = \lambda_2(1-C)P_{GG}(t) + P'_{GR}(t) - (\lambda_1+\mu_{p2})P_{GR}(t) + \mu_{C1}P_{FR}(t) + \mu_{P1}P_{RR}(t); \tag{27}$$

$$P'_{FR}(t+\Delta t) = \lambda_2(1-C)P_{GF}(t) + \lambda_1 CP_{GR}(t) + P'_{FR}(t) - (\mu_{c1}+\mu_{p2})P_{FR}(t); \tag{28}$$

$$P'_{RR}(t+\Delta t) = \lambda_2(1-C)P_{RG}(t) + \lambda_1(1-C)P_{GR}(t) + P'_{RR}(t) - (\mu_{p2}+\mu_{p1})P_{RR}(t); \tag{29}$$

By putting $P'(t+\Delta t)$, $P'(t)$, and other probability function derivatives equal to zero [26], t tends to ∞ in all differential equations [31] and solves the nine equations. The probability of the full working condition is computed by using the normalizing conditions [31,32], i.e.,

$$\sum_{i=0}^{64} Pi = 1; \tag{30}$$

The steady state availability of the [33] microgrid may be obtained as the summation of all nine working probabilities [33] obtained from Equation (30).

$$\begin{gathered} Availability = \mu_{c1}P_{GF}(t) + \mu_{p1}P_{RG}(t) + \mu_{c2}P_{FG}(t) + \mu_{p2}P_{GR}(t) - \\ (\lambda_1+\lambda_2)P_{GG}(t) + \lambda_1 CP_{GG}(t) - (\lambda_2+\mu_{c1})P_{GF}(t) + \\ \mu_{c2}P_{FF}(t) + \mu_{p2}P_{FR}(t) + \lambda_1(1-C)P_{GG}(t) - (\lambda_2+\mu_{p1})P_{RG}(t) + \\ \mu_{c2}P_{RF}(t) + \mu_{p2}P_{RR}(t) + \lambda_2 CP_{GF}(t) + \lambda_1 CP_{FG}(t) - (\mu_{c2} \\ +\mu_{c1})P_{FF}(t) + \lambda_2 CP_{RG}(t) + \lambda_1(1-C)P_{FG}(t) - (\mu_{c2}+\mu_{p1})P_{RF}(t) + \\ \lambda_2(1-C)P_{GG}(t) - (\lambda_1+\mu_{p2})P_{GR}(t) + \mu_{c1}P_{FR}(t) + \\ \mu_{p1}P_{RR}(t) + \lambda_2(1-C)P_{GF}(t) + \lambda_1 CP_{GR}(t) - (\mu_{c1}+\mu_{p2})P_{FR}(t) + \\ \lambda_2(1-C)P_{RG}(t) + \lambda_1(1-C)P_{GR}(t) - (\mu_{p2}+\mu_{p1})P_{RR}(t); \end{gathered} \tag{31}$$

The availability is evaluated based on different values of failure rates, repair rates, and *C* (i.e., coverage factor), and it is plotted concerning time using Equation (31).

6. Results and Discussion

The reliability of the microgrid was calculated concerning time using Markov modeling [29]. The total time considered was 150 years, and simulation iterations were set to 5000, so the delta per iteration was 0.3 times per division. At the moment the value of t is zero, corresponding to A(0), which is supposed to be the normal state, GG, of the system, then *S*(0) [26] is shown in Equation (32). Abbreviations are mentioned in the last section.

$$S(0) = [1;0;0;0;0;0;0;0;0;] \tag{31}$$

At $t = n.\Delta$ t, $S\ (n\ t) = A^n\ S(0)$, where $S(0)$ is the initial state, and accordingly, corresponding states are calculated by multiplying with the transition matrix.

The reliability computed with Markov modeling using Matlab code is shown in Figure 5. It was computed concerning time. As long as the system performs its defined task, it will increase its reliability, which is reduced concerning time. This has a very high impact on the electrical world, so microgrids should have high reliability to achieve their maximum benefits. The availability was computed by calculating the above availability Equations (16) to (25) above for various failure rates and repair rates. The failure rates and repair rates were varied, and the different values of availability were computed. Below is the availability computed concerning different values of failure rates when the repair rates were fixed i.e., 0.02, 0.08, 0.02, 0.02, and C is 0.8.

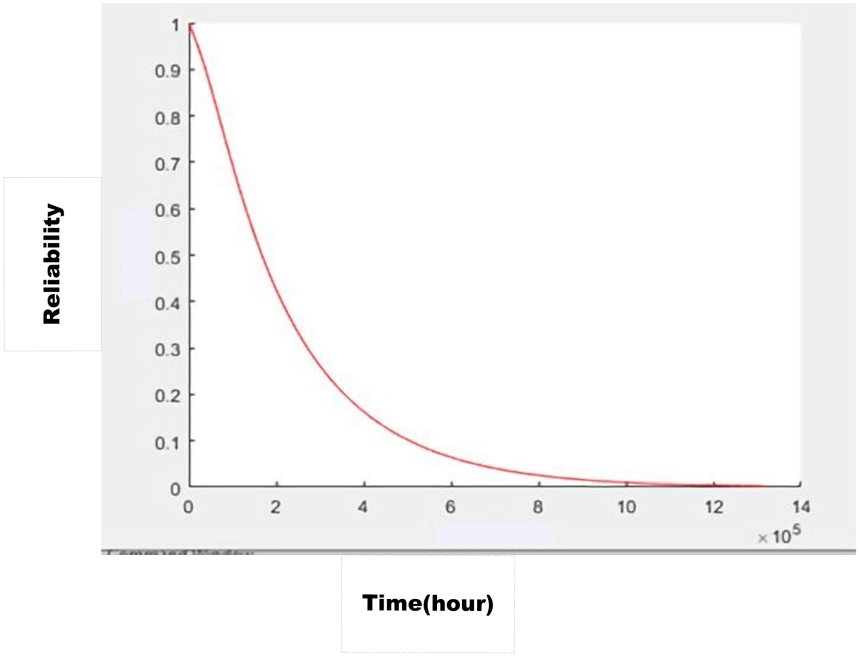

Figure 5. Bridge-linked PV panel configuration.

As shown in Figure 6, the availability increases concerning an increase in repair rate. It shows that the frequency of failure reduces, although the frequency of repair increases. The availability as well as reliability increases as compared to the baseline model of microgrid since the component's specific configuration impacts the increase in chances of a lifetime of the system and reduce the faults that occurred in that duration. During the design phase, the parameters of reliability and availability performance are considered for financial benefits, reducing the cost to microgrid owners.

6.1. Genetic Algorithms

The genetic technique is a natural selection and genetics-based search algorithm [34]. The genetic algorithm was used to optimize the results explained above. The objective function was maximizing concerning parameters. The parameters are the failure rates, of which different values are added; i.e., a range is defined and the optimum value is picked up to provide maximum reliability of the system [35]. The GA was set up with a range of variable values, and stopping criteria were also defined [36]. The initial population was created, which was iterated through generations. Mating was performed using single-point crossover. Then, the population was mutated, and new offspring and mutated chromosomes were evaluated. The results and associated parameters were sorted and statistics were performed [34]. Additionally, a neural network was trained successfully and helped to predict the data. In the reliability curve shown in Figure 4, a similar curve is shown to Figure 7's genetic algorithm results. It shows that reliability is highest in the initial years, but later becomes reduced; however, when we compare the duration of reliability, this effect completely diminishes, which is higher in the case of the genetic algorithm.

This took around 51 years, which is earlier than 26 years (i.e., mean time to failure). Thus, it can be concluded that genetic algorithms give better results compared to the Markov modeling-based reliability of a microgrid.

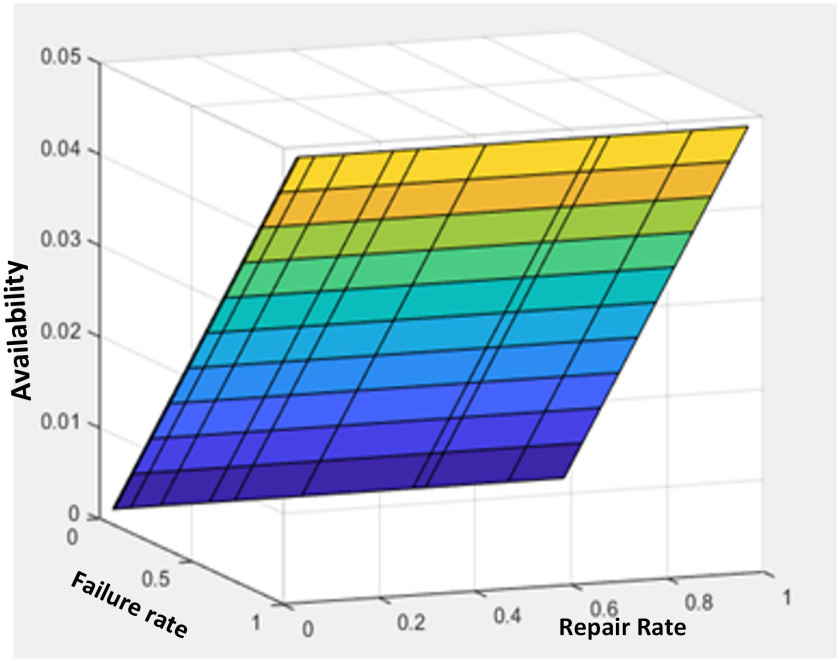

Figure 6. Availability concerning failure rate and repair rate.

The different range of performance parameters was varied from 0.1 to 0.9 to get the best possible results, as shown in Table 2, and specific values where reliability was highest were considered for the design of microgrid. The parameter used in the genetic algorithm computation is the bitstring population, which has been considered with single-point crossover. The mutation rate is 0.1, the crossover rate is 0.907, and the number of iterations are 51.

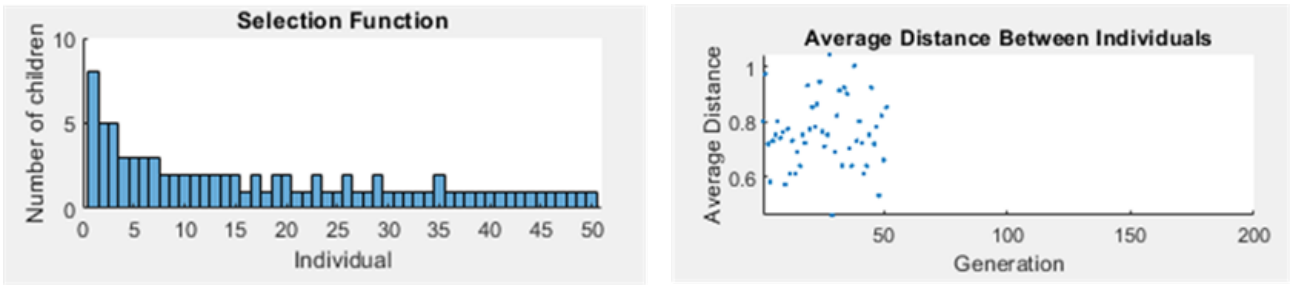

Figure 7. Genetic algorithm results.

Table 2. Parameter ranges.

Failure Rate or Repair Rate	Minimum	Maximum Value
λ_1	0.1	0.9
λ_2	0.1	1
λ_3	0.1	0.9
μ_1	0.1	0.5
μ_2	0.1	0.9
μ_3	0.1	0.7

6.2. Artificial Neural Networks

Artificial neural networks (ANN) come from the idea of natural biological neurons. As human neurons work based on their learning instead of fed code, similarly, an ANN works on data fed to it instead of logic. These networks are based on learning and do not follow any substantial equations. Only data required in terms of inputs and corresponding output generated from it are required, nothing else. An ANN enters the training process based on this data to learn and grasp the relationship between the input and output data [37]. Upon successful completion of training, an ANN can provide accurate output for any input variable without knowing the formula [38]. Therefore, the first step requires ANN data. This is the first major requirement for ANN implementation. Here, the data were collected by doing experiments. We collected data for 1000 output data with the following ranges of inputs: mean time to failures and mean time to repairs, which lies between zero to one. This means that the maximum and minimum ranges of the inputs were considered between 0 to 1. Matlab's random function was used to create varied numbers of samples inside the range to provide 1000 data samples. A new feed-forward neural network was introduced here along with the Minimax function. The input layer had six neurons, the hidden layer had five, and the output layer had one neuron for availability. The activation functions for the input, hidden, and output layers were logsig, tansig, and purelin, respectively. These activation functions were employed at the discretion of the user. At the start of the training, these activation functions were employed [39]. However, of all training algorithms, the Levenberg–Marquardt backpropagation algorithm is most commonly used for ANN training because it provides fast results in most cases. This training algorithm was the training algorithm by default. The ANN was initialized by the inputs, the output data, and these layers [40]. Despite not knowing the exact equation, an artificial neural network from its training can find the relationship between the input and output data [41]. The comparison of the three methods implemented is shown in Table 3.

Table 3. Parameter ranges.

Methods	MTTF (in Years)
Markov modelling	26
Genetic algorithm	51
Artificial networks	51.4

The present results indicate that the reliability and availability of microgrids decrease with time and concern higher values of failure rates, as shown in Figures 8 and 9 . The results are consistent when applied to the genetic algorithm as well as artificial neural networks, i.e., around 51 years and 51.4 years, respectively. The results of the further analysis indicate that fault frequency is highly reduced here; simultaneously, the frequency of repair is also increased. The present findings on the reliability and availability of microgrids shows significant improvement concerning previous findings with different values of failure rates and repair rates.

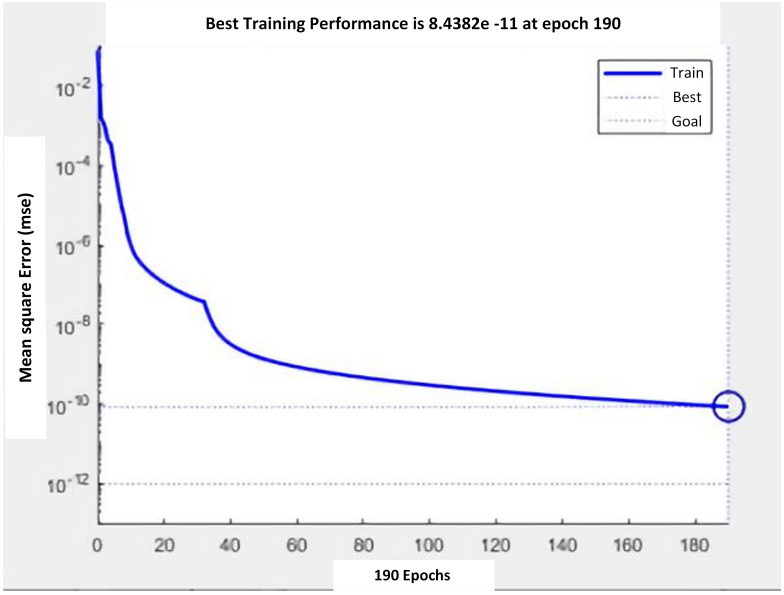

Figure 8. Artificial neural network results.

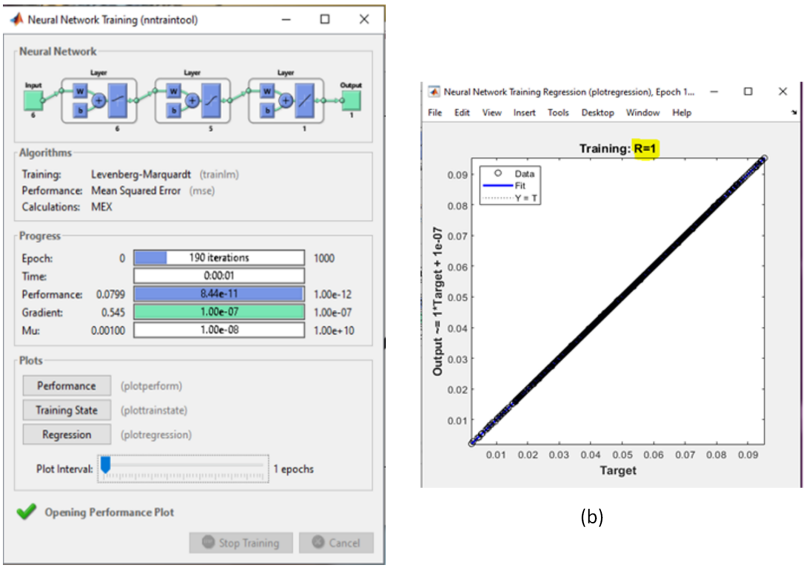

Figure 9. Artificial neural network results for a microgrid. (**a**) The model is trained for 1000 values using the Levenberg–Marquardt training method. (**b**) The output of the ANN after the model is fully trained.

7. Conclusions

This paper has investigated the reliability and availability of a microgrid based on different values of failure rates as well as repair rates that change with time, along with specific configurations of PV panels, using Markov modelling, GA and ANN to optimize MTTF. It is shown that ANN results are achieved in the shortest time of 7 s, obtaining an MTTF of 51.4 years and demonstrating the higher reliability and availability of the microgrid as compared to GA and Markov modeling. A better configuration and best possible values of failure rates and repair rates in designing the microgrid leads to almost double the overall microgrid's MTTF.

Possible future work is to use the same model on larger power and energy systems, along with an islanded mode, where all the submodels are isolated individually. New equipment is needed for studying the individual isolation of submodels to examine re-

liability with cost analysis. This work is conducted by studying physical components and submodels, but it can be extended by adding electronic communication devices (like Zigbee, wireless sensor networks, etc.) for the two-way flow of information and power.

Author Contributions: G.Y. studied a literature survey around microgrids and comes up with the idea of the development of microgrids which should be optimized using optimization methods and should be ready to implement in the real world. She has written this paper based on his finding and data is collected from real time implementation to get the optimal results. D.J. has added the idea of availability calculation based on the same data. D.J. contributed to the implementation of optimization techniques. L.G. and M.K.S. have contributed to the draft preparation and plagiarism check of this paper and resources availability. All authors have read and agreed to the published version of the manuscript.

Funding: This research received no external funding.

Institutional Review Board Statement: Not applicable.

Informed Consent Statement: Not applicable.

Data Availability Statement: Not applicable.

Acknowledgments: There is no support required from any institute or any funding agency for this study.

Conflicts of Interest: The authors declare no conflict of interest.

Abbreviations

The following abbreviations are used in this manuscript:

λ	Average failure rate
μ	Repair rate
MTTF	Mean time to failure
MTTR	Mean time to repair
ANN	Artificial neural networks
GA	Genetic algorithm
PV	Photovoltaic panels
Iot	Internet of things
R_{PV}	PV panel's reliability
T_j	Temperature at device junction
T_{HS}	Temperature at hot-spot for inductor
π_T	Function of T_j and T_{HS}
π_i	Factors that change the failure rate of submodels
π_Q	Fabrication factor
π_E	Environmental factor
π_S	Stress factor
π_C	Contact due to construction factor
λ_{MOSFET}	Failure rate of MOSFET
λ_{Diode}	Failure rate of diode
$\lambda_{Inductor}$	Failure rate of inductor
P_R	Probability of correct functioning of fault detection system
C	coverage factor
λ_c	Failure rate of core
λ_W	Failure rate of winding
λ_T	Failure rate of tank
λ_o	Failure rate of oil coating
λ_{SI}	Failure rate of solid insulation or solid coating
λ_B	Failure rate of bushing
λ_{TC}	Failure rate of tab changer
λ_P	Failure rate of cooling pump

λ_{CF}	Failure rate of cooling fan
P_{ij}	System-state transition probability from state i to state j
λ_k	Failure rate of kth element
μ_c	Recovery rate
μ_p	Maintenance rate

References

1. Wasiak, I.; Hanzelka, Z. Integration of distributed energy sources with electrical power grid. *Bull. Pol. Acad. Sci. Tech. Sci.* **2009**, *57*, 297–309. [CrossRef]
2. Ramabhotla, S.; Bayne, S.B. A Review on Reliability of Microgrid. In Proceedings of the Industrial and Commercial Power Systems Technical Conference, Las Vegas, NV, USA, 9 June–28 July 2020; pp. 1–9.
3. A Dark Year for Electricity Security, Reliability. 2021. Available online: https://www.powermag.com/2021-a-dark-year-for-electricity-security-reliability/ (accessed on 1 April 2022).
4. Green, R.C.; Wang, L.; Alam, M. Intelligent State Space Pruning with local search for power system reliability evaluation. In Proceedings of the 3rd IEEE PES Innovative Smart Grid Technologies Europe (ISGT Europe), Berlin, Germany, 14–17 October 2012; pp. 1–8.
5. Rana, M.; Li, L.; Su, S.W. Distributed State Estimation Over Unreliable Communication Networks with an Application to Smart Grids. *IEEE Trans. Green Commun. Netw.* **2017**, *1*, 89–96. [CrossRef]
6. Aghdam, F.H.; Hagh, M.T.; Abapour, M. Reliability Evaluation of Two-Stage Interleaved Boost Converter Interfacing PV Panels Based on Mode of Use. In Proceedings of the IEEE Transactions on Conference: 7th Power Electronics and Drive Systems, Technologies Conference (PEDSTC), Tehran, Iran, 16–18 February 2016.
7. Kim, S.; Kim, J. Reliability Evaluation of Distribution Network With DG Considering the Reliability of Protective Devices Affected by SFCL. *IEEE Trans. Appl. Supercond.* **2011**, *21*, 3561–3569. [CrossRef]
8. Miao, S.; Ning, G.; Gu, Y.; Yan, J.; Ma, B. Markov Chain model for solar farm generation and its application to generation performance evaluation. *J. Clean. Prod.* **2018**, *186*, 905–917. [CrossRef]
9. Abdelsamad, A.; Lubkeman, D. Reliability Analysis for a Hybrid Microgrid based on Chronological Monte Carlo Simulation with Markov Switching Modeling. In Proceedings of the IEEE Power & Energy Society Innovative Smart Grid Technologies Conference (ISGT), Washington, DC, USA, 18–21 February 2019; pp. 1–5.
10. Wei, C.; Shen, Z.; Xiao, D.; Wang, L.; Bai, X.; Chen, H. An optimal scheduling strategy for peer-to-peer trading in interconnected microgrids based on RO and Nash bargaining. *Appl. Energy* **2021**, *295*, 117024. [CrossRef]
11. Yang, J.; Su, C. Robust optimization of microgrid based on renewable distributed power generation and load demand uncertainty. *Energy* **2021**, *223*, 120043. [CrossRef]
12. Xiao, D.; do Prado, J.C.; Qiao, W. Optimal joint demand and virtual bidding for a strategic retailer in the short-term electricity market. *Electr. Power Syst. Res.* **2021**, *190*, 106855. [CrossRef]
13. Tuffaha, T.; Almuhaini, M. Reliability assessment of a microgrid distribution system with pv and storage. In Proceedings of the International Symposium on Smart Electric Distribution Systems and Technologies (EDST), Vienna, Austria, 8–11 September 2015; pp. 195–199.
14. Kumar, R.; Tewari, P.C.; Khanduja, D. Parameters optimization of fabric finishing system of a textile industry using teaching–learning-based optimization algorithm. *Int. J. Ind. Eng. Comput.* **2018**, *9*, 221–234. [CrossRef]
15. He, J.; Xiao, X.; Zhong, R.; Huang, W.; Li, D.; Chen, Q. New AC & DC hybrid power supply system and its reliability analysis in data centre. *J. Eng.* **2019**, *20*, 2800–2803.
16. Saraswat, S.; Yadava, G.S. An overview on reliability, availability, maintainability and supportability (RAMS) engineering. *Int. J. Qual. Reliab. Manag.* **2008**, *25*, 330–344. [CrossRef]
17. Sayed, A.; El-Shimy, M.; El-Metwally, M.; Elshahed, M. Reliability, availability and maintainability analysis for grid-connected solar photovoltaic systems. *Energies* **2019**, *12*, 1213. [CrossRef]
18. Andalib-Bin-Karim, C.; Liang, X.; Chowdhury, H.-U.A. Generation Reliability Assessment of Stand-Alone Hybrid Power System—A Case Study. In Proceedings of the 2017 IEEE International Conference on Industrial Technology (ICIT), Toronto, ON, Canada, 22–25 March 2017; pp. 434–439.
19. Gautam, N.K.; Kaushika, N.D. Reliability evaluation of solar photovoltaic arrays. *Sol. Energy* **2002**, *72*, 129–141. [CrossRef]
20. Yao, B.; Chen, H.; He, X.Q.; Xiao, Q.Z.; Kuang, X.J. Reliability and failure analysis of DC/DC converter and case studies. In Proceedings of the 2013 International Conference on Quality, Reliability, Risk, Maintenance, and Safety Engineering, Chengdu, China, 15–18 July 2013; pp. 1133–1135.
21. Javadian, V.; Kaboli, S. Reliability assessment of some high side MOSFET drivers for buck converter. In Proceedings of the 3rd International Conference on Electric Power and Energy Conversion Systems, Istanbul, Turkey, 2–4 October 2013; pp. 1–6.
22. Asl, E.S.; Sabahi, M.; Abapour, M.; Khosroshahi, A.E.; Khoun-Jahan, H. Markov Chain Modeling for Reliability Analysis of Multi-Phase Buck Converters. *J. Circuits Syst. Comput.* **2020**, *29*, 2050139. [CrossRef]
23. Defence, Military Handbook: Reliability Prediction of Electronic Equipment: MIL-HDBK-217F: 2 December 1991: Department of Defence. 1991. Available online: http://everyspec.com/MIL-HDBK/MIL-HDBK-0200-0299/MIL-HDBK-217F_14591/ (accessed on 1 April 2022).

24. Singh, A.; Patil, A.J.; Tripathi, V.K.; Sharma, R.K.; Jarial, R.K. Reliability Modelling and Simulation for Assessment of Electric Arc Furnace Transformers. In Proceedings of the 2020 IEEE International Conference on Computing, Power and Communication Technologies (GUCON), Pune, India, 29–30 October 2021; pp. 239–244.
25. Agarwal S.S.; Kansal, M.L. Fuzzy fault tree analysis of a power transformer. In Proceedings of the 2012 International Conference on Quality, Reliability, Risk, Maintenance, and Safety Engineering, Chengdu, China, 15–18 June 2012; pp. 1000–1004.
26. Binh, P.T.T.; Khoa, T.Q.D. Application of Fuzzy Markov in calculating reliability of power systems. In Proceedings of the IEEE/PES 604 Transmission & Distribution Conference and Exposition: Latin America, Caracas, Venezuela, 15–18 August 2006; pp. 1–4. [CrossRef]
27. Tewari, P.C.; Khanduja, R.; Gupta, M. Performance enhancement for crystallization unit of a sugar plant using genetic algorithm technique. *J. Ind. Eng. Int.* **2012**, *8*, 1. [CrossRef]
28. Kumar, A.; Kumar, P. Application of Markov process/mathematical modelling in analysing communication system reliability. *Int. J. Qual. Reliab. Manag.* **2020**, *37*, 354–371. [CrossRef]
29. Manglik, M.; Rawat, N.; Ram, M. Reliability and Availability analysis of a cloud computing transition system under multiple failures. *Int. J. Qual. Reliab. Manag.* **2020**, *37*, 6–7. [CrossRef]
30. Cevasco, D.; Koukoura, S.; Kolios, A.J. Reliability, availability, maintainability data review for the identification of trends in offshore wind energy applications. *Renew. Sustain. Energy Rev.* **2021**, *136*, 110414. [CrossRef]
31. Gupta, S. Stochastic modelling and availability analysis of a critical engineering system. *Int. J. Qual. Reliab. Manag.* **2019**, *36*, 782–796. [CrossRef]
32. Gupta, S.; Tewari, P. Simulation Model for Stochastic Analysis and Performance Evaluation of Condensate System of a Thermal Power Plant. *Bangladesh J. Sci. Ind. Res.* **1970**, *44*, 387–398. [CrossRef]
33. Xiang, Y.; Wang, L.; Fu, T. A preliminary study of power system reliability considering cloud service reliability. In Proceedings of the 2014 International Conference on Power System Technology, Chengdu, China, 20–22 October 2014; pp. 2031–2036. [CrossRef]
34. Joshi, D.; Sandhu, K.S. Excitation control of self excited induction generator using genetic algorithm and artificial neural network. *Int. J. Math. Model. Methods Appl. Sci.* **2009**, *3*, 68–75.
35. Joshi, D.; Sandhu, K.S.; Bansal, R.C. Steady-state analysis of self-excited induction generators using genetic algorithm approach under different operating modes. *Int. J. Sustain. Energy* **2013**, *32*, 248–253. [CrossRef]
36. Mohamed, F.A.; Koivo, H.N. Online management genetic algorithms of microgrid for residential application. *Energy Conv. Manag.* **2012**, *64*, 562–568. [CrossRef]
37. Lopez-Garcia, T.B.; Coronado-Mendoza, A.; Domínguez-Navarro, J.A. Artificial neural networks in microgrids: A review. *Eng. Appl. Artif. Intell.* **2020**, *95*, 103894. [CrossRef]
38. Vogt, T.; Weber, D.; Wallscheid, O.; Bocker, J. Prediction of residual power peaks in industrial microgrids using artificial neural networks. In Proceedings of the 2017 International Joint Conference on Neural Networks (IJCNN), Anchorage, AK, USA, 14–19 May 2017; pp. 3228–3235.
39. Macedo, M.N.Q.; Galo, J.J.M.; de Almeida, L.A.L.; De, A.C. Demand side management using artificial neural networks in a smart grid environment. *Renew. Sustain. Energy Rev.* **2015**, *41*, 128–133. [CrossRef]
40. Ronay, K.; Bica, D.; Munteanu, C. Micro-grid Development Using Artificial Neural Network for Renewable Energy Forecast and System Control. *Procedia Eng.* **2017**, *181*, 818–823. [CrossRef]
41. MacDougall, P.; Kosek, A.M.; Bindner, H.W.; Deconinck, G. Applying machine learning techniques for forecasting flexibility of virtual power plants. In Proceedings of the 2016 IEEE Electrical Power and Energy Conference, Ottawa, ON, Canada, 12–14 October 2016; pp. 1–6.